The analysis of liquid structure data from time-of-flight neutron diffractometry

1989 J. Phys.: Condens. Matter 1 3433

(http://iopscience.iop.org/0953-8984/1/22/005)

J. Phys.: Condens. Matter 1 (1989) 3433–3451. Printed in the UK

The analysis of liquid structure data from time-of-flight neutron diffractometry

M A Howe†‡, R L McGreevy† and W S Howells§

† Clarendon Laboratory, Parks Road, Oxford OX1 3PU, UK

§ Neutron Division, Rutherford Appleton Laboratory, Chilton, Oxon OX11 0QX, UK

Received 26 October 1988, in final form 17 January 1989

Abstract. We discuss in detail the analysis of structural data on liquids obtained using time-of-flight neutron diffractometry, in particular the Liquids and Amorphous Materials Diffractometer (LAD) situated at the ISIS pulsed neutron source at the Rutherford Appleton Laboratory. A series expansion for the inelasticity corrections has been calculated to higher order than has been done before and it is shown that the new terms are significant. It is argued, however, that there are fundamental reasons why any such correction will be inadequate for the lowest-energy neutrons. The problem of combining the results from detectors at different angles is considered and we present a generally applicable method for doing this in such a way that the effect of instrumental resolution is readily included. These procedures are demonstrated and tested on data obtained in an experiment to measure the structure factor of molten CsCl at 670°C, close to the melting point, and at 970°C using LAD. The result at the lower temperature is in good agreement with a previous result obtained using the D4 steady state diffractometer at the High Flux Reactor of the Institut Laue–Langevin, Grenoble. The change in the structure factor between the two temperatures can be accounted for entirely in terms of density scaling indicating that there is little, if any, change in the pair correlation function $g(r)$ as the temperature is raised.

1. Introduction

For many years now the structures of liquids and amorphous materials have been studied by neutron diffraction. Most of these experiments have taken place using conventional reactor-based diffractometers which measure the scattered intensity of a monochromatic beam of neutrons as a function of scattering angle. An example of such an instrument is D4B (formerly D4) at the Institut Laue–Langevin (ILL), Grenoble. The methods of data correction and analysis necessary to obtain the total neutron weighted structure factor, $F(Q)$, from data so obtained are now well established (see, for example, Howe (1987) or Locke *et al* (1985) and references therein) and, with minor variations in detail, are used universally. Some experiments, however, have used time-of-flight diffractometers such as the Total Scattering Spectrometer (TSS) on the Harwell LINAC (Wright *et al* 1985) or the General Purpose and Special Environment Powder Diffractometers (GPPD and SEPD) at the Intense Pulsed Neutron Source (IPNS) of the Argonne National Laboratory, USA (Wood *et al* 1988, Saboungi *et al* 1987) in which the scattering of a pulse of neutrons, of a wide range of energies, is measured as a function of time of flight at a small number of scattering angles. With

‡ Current address: Chemical Technology Division, Argonne National Laboratory, 9700 South Cass Avenue, Argonne, Illinois 60439-4837, USA.

0953-8984/89/223433+19$02.50

the advent of the high flux pulsed neutron source ISIS at the Rutherford Appleton Laboratory and its Liquids and Amorphous Materials Diffractometer (LAD) and the recent increase in intensity of IPNS and the commisioning of their Glasses, Liquids and Amorphous Materials Diffractometer (GLAD) this type of diffractometry has become more important.

Although the basic correction procedures for time-of-flight diffraction have been worked out and applied (Price 1982, Howells *et al* 1985, Howells 1986), with the large amount of data of high statistical quality that will now be produced the smaller details of the corrections become important. It is then perhaps timely to consider some of these details anew and to provide some discussion of the remainder.

In this paper we discuss in some detail analysis of time-of-flight neutron diffraction data and describe the procedures we have used to analyse data from LAD. In so doing we extend the series expansion of Powles (1973) for the inelasticity, or Placzek, correction to higher order and show that the new terms are significant. We also discuss the validity of such an expansion. After correction of the data we are left with a number of spectra each of which represents $F(Q)$ over a different Q-range and it is usually necessary to combine these in some way. We describe a method of doing this in such a way that the effect of instrumental resolution is readily included. We demonstrate our methods by applying them to an experiment on molten caesium chloride.

The structures of many alkali and alkaline earth chlorides close to their melting points have now been determined in detail (McGreevy 1987). However nothing is known of the temperature dependence of this structure, except in the case of $CaCl_2$ in which a close Ca–Ca grouping seems to break up as the temperature is raised (Day and McGreevy 1985). The purpose of the present experiment (which was one of the first to use LAD) was to see if there was any significant change in structure over the temperature range we could obtain, and to compare the result at the lower temperature with that obtained by Locke *et al* (1985) using D4 at ILL. There is no change in the shape of the Raman scattering spectrum of CsCl with temperature (Fairbanks 1987) which contrasts with the case of $CaCl_2$ (Bunten *et al* 1984) and may indicate that there is little change in structure.

The comparison with reactor data is, in part, a test of the efficacy of our correction procedure. However, matters are not quite as simple as that. Because of inelasticity effects, among other things, all neutron diffraction instruments determine only an approximation to $F(Q)$, and different instruments will give different approximations. This has been demonstrated for molten CsCl by Fairbanks and McGreevy (1989) and one of its consequences is shown by the work of Howe and McGreevy (1988) on molten LiCl. Our comparison is therefore also of the approximations to $F(Q)$ obtained by the two instruments.

2. The experiment

The diffractometer LAD has been described in detail elsewhere (Howells 1980, *ISIS User Guide* 1988). The detectors are arranged such that on each side of the instrument there are four at a scattering angle of 150°, and one at each of the angles 90°, 58°, 35°, 20°, 10°, and 5°. At the time of this experiment those at 20°, 35°, and 58° on one side of the instrument were scintillation detectors and the remainder were helium gas detectors. Spectra were recorded separately for each of these detectors and also for a

monitor in the incident beam and a transmission monitor, making a total of 22 spectra in all.

The sample was contained in a vanadium cylinder of internal radius 0.45 cm and external radius 0.49 cm. The height of the sample in the container when molten was greater than the height of the neutron beam which was 3 cm. The width of the beam was 1.5 cm. A cylinder of vanadium foil, concentric with the sample and through which an electric current was passed, provided the heating.

Spectra were recorded for the sample at 670°C and at 970°C, for an empty container at 670°C, and for the background (the empty furnace) and a vanadium rod of 10 mm diameter both at room temperature. Those for a scattering angle of 90° are shown in figure 1. The sharp dip at approximately 300 ms in the spectrum for CsCl is caused by an absorption resonance of caesium at 6 eV.

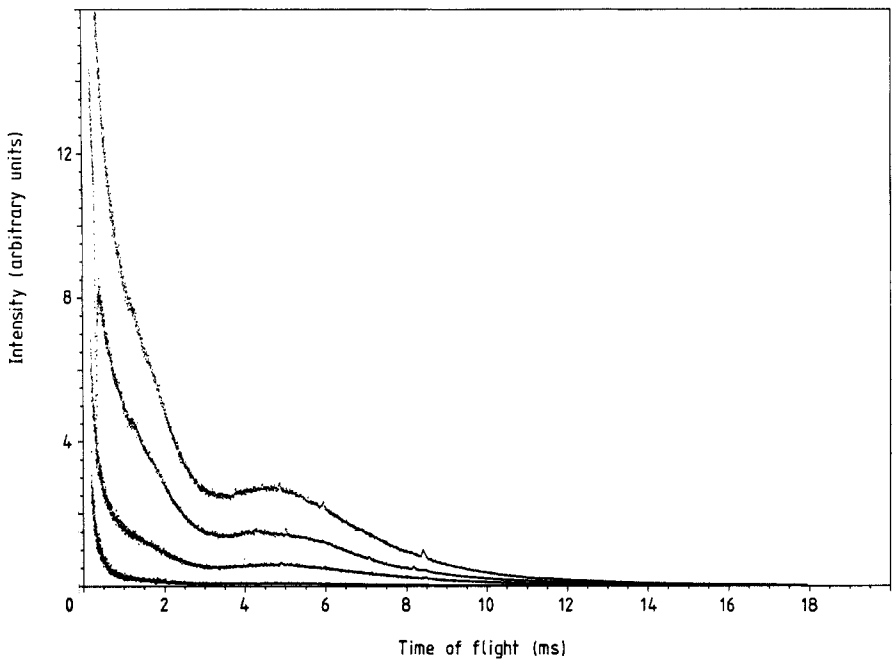

Figure 1. Normalised scattering intensities at an angle of 90° for (from top to bottom) the vanadium rod at room temperature, molten caesium chloride at 670°C, the empty container at 670°C, and the empty furnace at room temperature.

3. Data analysis

We start with five data sets consisting of raw data for the sample at two temperatures, the can, the background, and a vanadium rod. For each of these the raw data is in the form of a number of spectra, one for each detector, consisting of counts as a function of time of flight. The analysis of this passes through a number of stages.

(1) For each data set data from equivalent detectors are summed and normalised by monitor count.

(2) Each sample and vanadium spectrum is corrected for background and container scattering and for attenuation.

(3) The vanadium spectra are corrected for multiple scattering and used to put the sample spectra on an absolute scale. The sample spectra are then also corrected for multiple scattering.

(4) The inelasticity correction is applied to the sample spectra which are now expressed as a function of Q, the momentum transfer.

(5) The different spectra are combined, taking into account the effect of instrumental resolution, to produce $F(Q)$ and the total (neutron weighted) pair correlation function $h_T(r)$.

These stages will now be discussed in more detail in the corresponding subsections below.

3.1. Summing equivalent detectors

We start with a large amount of data which it is desirable to reduce to more manageable proportions. To do this we sum the spectra from detectors that are considered equivalent, having checked them for consistency by comparing the ratio of sample counts to vanadium counts for all of the spectra to be summed. In our case we summed the pairs of detectors at 5°, 10° and 90°. The two detectors at 20° are not equivalent as the corrections are slightly different for gas and scintillation detectors so they have not been summed. The same is true for the pairs at 35° and 58° although the scintillation detector at 35° was not working correctly so that has been ignored entirely. We also omitted the eight spectra at a scattering angle of 150° from the analysis because, for our sample, there is little structure in the range of momentum transfer they cover and, because of the poor statistics, we considered that they contained little useful information.

The number of neutrons counted depends on the total number of neutrons that have been incident on the sample. To remove this dependency every spectrum of each data set is divided by the total monitor count (monitor count integrated over time of flight). It is convenient at this stage to express the spectra as a function of neutron wavelength, assuming that neutrons are scattered elastically. The wavelength of elastically scattered neutrons is given by

$$\lambda_e = 2\pi\hbar t/m(d_1 + d_2) \tag{1}$$

where t is the time of flight, m the neutron mass, d_1 the distance from the moderator to the sample (10 m), and d_2 the distance from the sample to the detector (1.043 m).

3.2. Attenuation corrections

The scattering intensity from the sample is modified by background and container scattering, by attenuation in the sample and container, and by multiple scattering. It is possible to write a neutron transport equation in which all these effects are included (Sears 1975). However the solution of such an equation is in general not straight forward unless a Monte Carlo method is used, and this can be time consuming. Instead we assume that we can consider attenuation and multiple scattering separately. In so doing we are making two approximations: (i) that multiply scattered neutrons are attenuated by the same amount as singly scattered neutrons; and (ii) that no neutrons

are scattered in both sample and container. The second of these approximations will be good for a thin-walled container such as we have here but if a thick-walled container had been used it would not be and the use of a Monte Carlo method (Bischoff *et al* 1972, Copley 1974, Mildner *et al* 1977, Mildner and Carpenter 1977) would be more appropriate. We write the experimentally observed scattering intensities from vanadium, sample, container, and background (I_V^E, I_S^E, I_C^E, and I_B^E respectively) in terms of nominal unattenuated intensities (I_V etc) and attenuation coefficients (A_{VV} etc):

$$I_V^E = A_{VV}I_V + I_B \qquad I_S^E = A_{SSC}I_S + A_{CSC}I_C + I_B$$
$$I_C^E = A_{CC}I_C + I_B \qquad I_B^E = I_B \tag{2}$$

The first subscript of the attenuation coefficients indicates the scattering being attenuated while the remainder show what is causing the attenuation. Thus A_{CSC} is the attenuation of container scattering by container and sample while A_{CC} is the attenuation of container scattering by the container only. Solution of these equations gives

$$I_V = (I_V^E - I_B^E)/A_{VV}$$
$$I_S = \frac{1}{A_{SSC}}\left[I_S^E - \frac{A_{CSC}}{A_{CC}}I_C^E - \left(1 - \frac{A_{CSC}}{A_{CC}}\right)I_B^E\right]. \tag{3}$$

Thus we can calculate $I_V(\lambda_e)$ and $I_S(\lambda_e)$ for each of the scattering angles provided we can calculate the attenuation coefficients, which also depend on scattering angle and, through their dependence on scattering and absorption cross sections, on wavelength. We have used for this calculation a routine written by Poncet (1977), which is based on the method of Paalman and Pings (1962) for a cylindrical sample within a cylindrical container. Different routines must be used for different geometries or for non-uniform beam profiles (e.g. Soper and Egelstaff 1980). In doing this calculation we have assumed that the absorption cross sections were proportional to neutron wavelength so that they could be calculated from the values given in table 1. This is generally true for thermal neutrons but is not valid near a nuclear resonance. Because the data cannot be corrected properly near the caesium resonance we will not be able to use data gathered with high-energy neutrons.

Table 1. Neutron scattering properties, taken from Lovesey (1984). Thermodynamic properties, taken from Janz (1967) are as follows: melting point, 645°C; ρ(670°C), 0.019 79 Å^{-3}; ρ(970°C), 0.017 49 Å^{-3}; isothermal compressibility at 700°C, 4.29×10^{-4} cm^3 J^{-1}.

	Cs	Cl
$\bar{b}$ (10^{-12} cm)	0.542	0.9579
$\overline{b^2}$ (10^{-24} cm^2)	0.315	1.323
σ_a at 2200 m s^{-1} (b)	29	33.5

Another approach would be to calculate the attenuation coefficients as a function of wavelength using the measured attenuation of unscattered neutrons determined using the transmission monitor. This method has the advantage that it allows for variation in

the cross sections with neutron energy of a form other than that expected; it has been used successfully by Soper (1988). However, data in the region of a nuclear resonance still could not be easily interpreted because the coherent neutron scattering lengths are no longer constant.

3.3. Multiple scattering and calibration

Neglecting, for a moment, multiple scattering, the intensity at a given scattering angle is

$$I_S(\lambda_e) = N_S \int d\lambda\, \phi(\lambda)\epsilon(k')\frac{k'}{k}S(Q,\omega)\left(\frac{d\omega}{d\lambda_e}\right) \tag{4}$$

where the integration is over the incident spectrun $\phi(\lambda)$ at constant λ_e, k and k' are the incident and scattered wavevectors respectively, $\epsilon(k')$ describes the efficiency of the detector and N_S is the number of sample atoms. $S(Q,\omega)$ is the total neutron weighted dynamic structure factor, $Q = (4\pi/\lambda)\sin(\theta/2)$, where θ is the scattering angle, is the momentum transfer, and $\hbar\omega$ is the energy loss, of the scattered neutrons. In the static approximation $S(Q,\omega) = S(Q)\delta(\omega)$ and this reduces to

$$I_S(\lambda_e) = N_S\Phi(\lambda_e)S(Q) \tag{5}$$

where, for convenience, we have introduced $\Phi(\lambda_e)$. Including multiple scattering this becomes

$$\begin{aligned} I_S(\lambda_e) &= N_S\Phi(\lambda_e)(S(Q) + \overline{b_S^2}\Delta_S) \\ &= N_S\Phi(\lambda_e)\left(\overline{b_S^2}(1+\Delta_S) + \sum_\alpha\sum_\beta c_\alpha c_\beta \bar{b}_\alpha \bar{b}_\beta (A_{\alpha\beta}(Q) - 1)\right) \end{aligned} \tag{6}$$

where $\overline{b_S^2}$, $\bar{b}_\alpha$ and $\bar{b}_\beta$ are neutron scattering lengths, Δ_S is the multiple scattering fraction, the sums are over particle type, c_α is the fractional concentration of particles of type α and $A_{\alpha\beta}(Q)$ is a Faber–Ziman partial structure factor. In the case of vanadium the scattering is almost totally incoherent and $\bar{b}_V$ is very small. The coherent scattering, which gives rise to a few small Bragg peaks, can be removed by smoothing the spectra using cubic splines to give the smoothed intensity $\bar{I}_V(\lambda_e)$:

$$\bar{I}_V(\lambda_e) = N_V\Phi(\lambda_e)(\overline{b_V^2} - \bar{b}_V^2 + \overline{b_V^2}\Delta_V) \tag{7}$$

so the total structure factor for the sample is

$$S(Q) = \frac{N_V}{N_S}\frac{I_S(\lambda_e)}{\bar{I}_V(\lambda_e)}[\overline{b_V^2}(1+\Delta_V) - \bar{b}_V^2] - \overline{b_S^2}\Delta_S \tag{8}$$

which we express as a function of momentum transfer. The multiple scattering, Δ_V and Δ_S, was estimated by interpolating the tabulated data of Howe (1987) (which is in good agreement with that of Sears (1975)) and was assumed to be independent of scattering angle although dependent on wavelength. Monte Carlo calculations (Howe 1987) show that this is a good approximation for samples of the shape, size, and absorption of ours.

3.4. Inelasticity corrections

In the previous section we used the static approximation but for a liquid the atoms recoil when scattering neutrons and the scattering is not purely elastic. $S(Q)$ is the integral of $S(Q,\omega)$ over ω at constant Q but the result of the experiment is the integral in (4). This can also be written as an integral over ω (Powles 1973):

$$I_S(Q_e) = N_S\Phi(Q_e)\int C\frac{\lambda}{\lambda_e}\frac{\phi(\lambda)}{\phi(\lambda_e)}\frac{\epsilon(k')}{\epsilon(k_e)}\frac{k'}{k}S(Q,\omega)\,d\omega \tag{9}$$

at constant λ_e where we have introduced $Q_e = 4\pi/\lambda_e \sin(\theta/2)$ and

$$C = \frac{d_1 + d_2(1-2m\omega/\hbar k^2)^{-1/2}}{d_1 + d_2(1-2m\omega/\hbar k^2)^{-3/2}} \tag{10}$$

We see that (9) is an integral of $S(Q,\omega)$ multiplied by a function of ω performed along a path that is not at constant Q. There is a difference between this and the integral that defines $S(Q)$ and in order to correctly determine the structure factor we must make a correction for this difference. Such a correction is known as the inelasticity, or Placzek, correction. It is clear that to calculate this exactly we must have a full knowledge of $S(Q,\omega)$ but if we had then of course we would know $S(Q)$ already. There are various approaches to this problem. Some authors have used a model of $S(Q,\omega)$ or a combination of an experimentally determined $S(Q,\omega)$ and a model (Dahlborg and Kunsch 1983). The disadvantage of the latter is that it requires good experimental data; and both have the disadvantage that they depend on the details of the model which can only be an approximation. Another approach is to use a power series expansion that can express the correction in terms of the moments of $S(Q,\omega)$. The first few moments are known; the terms containing the higher moments, which depend on the potential, are neglected. This is the approach used by Placzek (1952) and which, in the form developed by Yarnell *et al* (1973), is often used for reactor data.

If the integrand in (9) is expressed as a power series in ω the zeroth-order term will reduce to (5) and we get

$$I_S(Q_e) = N_S\Phi(Q_e)(S(Q_e) + P_1(Q_e) + P_2(Q_e) + \ldots) \tag{11}$$

and (8) becomes

$$S(Q_e) = \frac{N_V}{N_S}\frac{I_S(\lambda_e)}{\bar{I}_V(\lambda_e)}[\overline{b_V^2}(1+\Delta_V) - \bar{b}_V^2] - \overline{b_S^2}\Delta_S - P_1(Q_e) - P_2(Q_e) - \ldots \tag{12}$$

where $P_1(Q_e)$ and $P_2(Q_e)$ are the first- and second-order terms of the inelasticity correction, respectively. The first-order term was calculated by Powles (1973). In Appendix 1 we extend the calculation so as to determine the second-order term. For this series expansion approach to be useful the series giving the correction must be dominated by the terms that have not been neglected. In figure 2 we show the correction to first order and to second order; it can be seen that they are quite different, which suggests that the first-order term alone is inadequate. With the inclusion of the second-order term we see that the correction diverges at low Q_e because of the k_BT/E term. This behaviour can be understood by considering the paths along which the integration is performed and which are shown in figure 3. For high values of Q_e the integration in nearly at constant Q but at low Q_e as Q_e decreases the paths become

increasingly shallow and the value of the integral will increase due to contributions from the broader quasi-elastic peak at higher Q. This is demonstrated by the third curve shown in figure 2, which is obtained by performing the integration in (9) using an $S(Q,\omega)$ for a free particle of mass equal to the mean of the caesium and chlorine atomic masses. It is clear that the expansion to second order is a better representation of this than the expansion to first order although there are significant differences particularly at large scattering angles. We conclude that the expansion to first order is of little use and that even the expansion to second order may be of limited accuracy at low Q. At high Q, on the other hand, the inelasticity correction is very small.

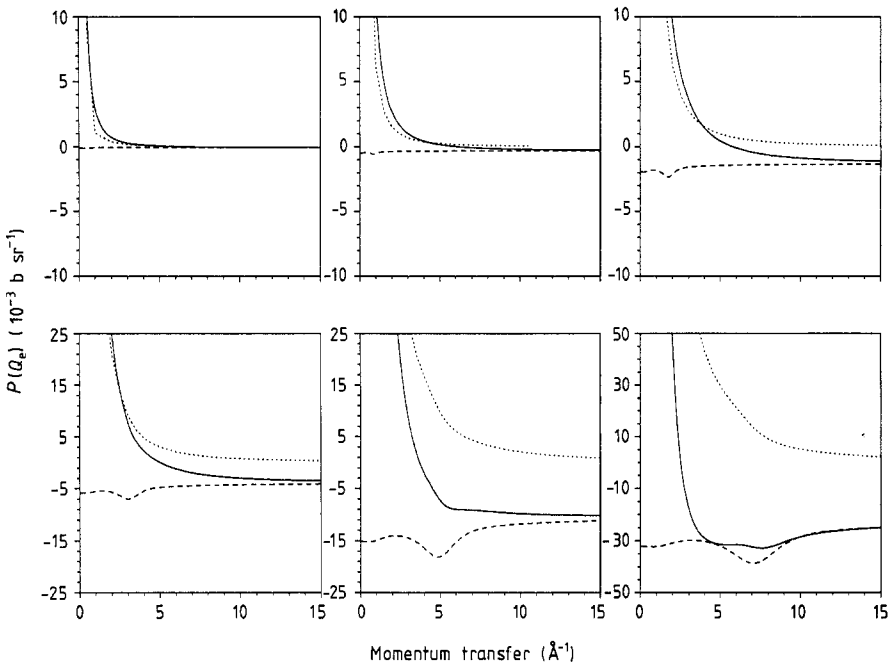

Figure 2. Inelasticity corrections at angles of (from left to right, top to bottom) 5°, 10°, 20°, 35°, 58°, and 90°. The broken curves are the expansion to first order ($P_1(Q_e)$);the full curves are the expansion to second order ($P_1(Q_e) + P_2(Q_e)$); and the dotted curves are obtained by integration of a free particle $S(Q,\omega)$.

We can also see from figure 3 that at low Q_e the slopes of the paths are similar to the velocity of sound in many liquids. As has been discussed by Fairbanks and McGreevy (1989), this can result in an increase in scattering at low Q_e due to scattering from acoustic-phonon-like modes. As such collective modes do not contribute to the first two moments of $S(Q,\omega)$ the series expansion we have derived cannot be expected to correct for this effect.

The inelasticity correction contains terms in the incident flux, the detector efficiency, and their derivatives. For the flux we fitted the expression (Howells 1984)

$$\phi(\lambda) = \phi_{\mathrm{Max}} \frac{\lambda_T^4}{\lambda^5} \exp\left[-\left(\frac{\lambda_T}{\lambda}\right)^2\right] + \frac{\phi_{\mathrm{epi}}}{\lambda^{1+2a}} \frac{1}{1+\exp[(\lambda-\lambda_1)/\lambda_2]} \tag{13}$$

where ϕ_{Max}, ϕ_{epi}, λ_T, λ_1, λ_2 and a are variable parameters, to the incident flux after it had been corrected for the efficiency of the monitor; for the efficiency we used

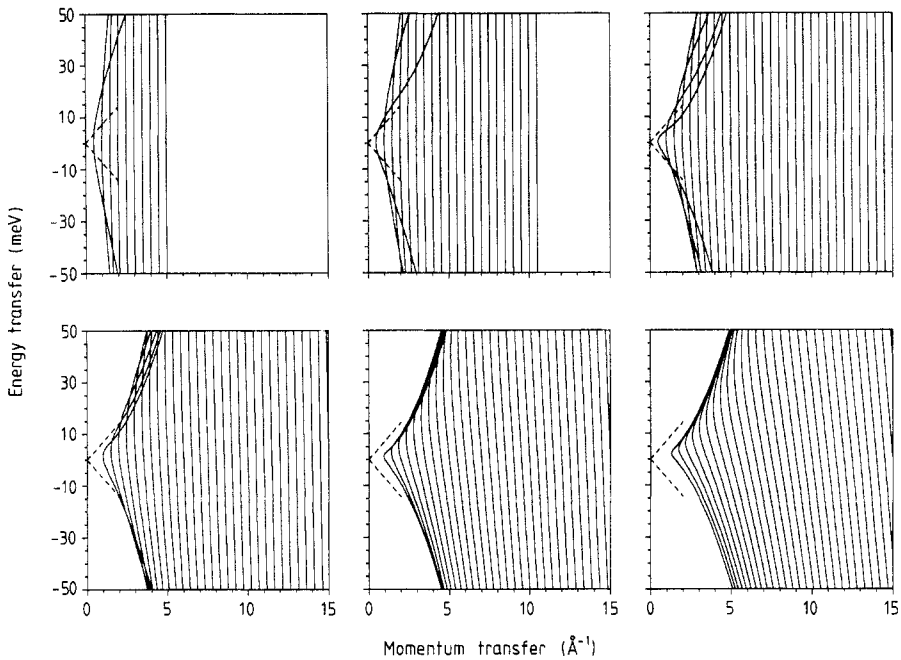

Figure 3. Integration paths for the LAD detectors at angles of (from left to right, top to bottom) 5°, 10°, 20°, 35°, 58°, and 90°. The broken lines represent the velocity of sound in molten CsCl at 670°C.

the expression $\epsilon = 1 - \exp(-\alpha\lambda)$ where $\alpha = 0.83$ for the scintillation detectors and $\alpha = 1/1.44$ for the gas detectors.

After applying the inelasticity corrections we now have, for each sample, eight spectra, each of which is an approximation to $S(Q)$ (we now drop the subscript of Q_e for convenience) over a different range of momentum transfer. Six of those at 670°C are shown in figure 4. The effect of the caesium resonance can be quite clearly seen in the results from the lower angles: there is a fairly broad dip in the spectra at their high-Q ends. At the low-Q ends considerable differences can be seen between the spectra. This is probably mainly due to inelasticity effects because, as we have discussed above, the correction cannot be considered very reliable at low Q. However there are also other possible factors. The low-Q data are obtained using long-wavelength neutrons, the flux of which is low and the background relatively high. The absorption at these wavelengths is fairly high and so the absorption corrections are large. If the background was in part sample dependent this would have the largest effect in this region.

Because of these problems it was necessary to truncate the spectra. All data at Q-values greater than that corresponding to a neutron energy of 1 eV were discarded. The value of 1 eV was chosen in order to remove all evidence of the resonance dip from the spectra. The maximum Q-value of the remaining data was 32 $Å^{-1}$ which is still far larger than that at which no structure is observable in $S(Q)$. At the low-Q end the spectra were truncated at the Q-values 0.3 $Å^{-1}$ (5°), 1.5 $Å^{-1}$ (10°), 2.5 $Å^{-1}$ (20°), 3 $Å^{-1}$ (35°), 4 $Å^{-1}$ (58°) and 5 $Å^{-1}$ (90°) (corresponding to energies between 50 meV and 300 meV) which were chosen somewhat arbitrarily so that the spectra now agreed with each other in the regions of overlap.

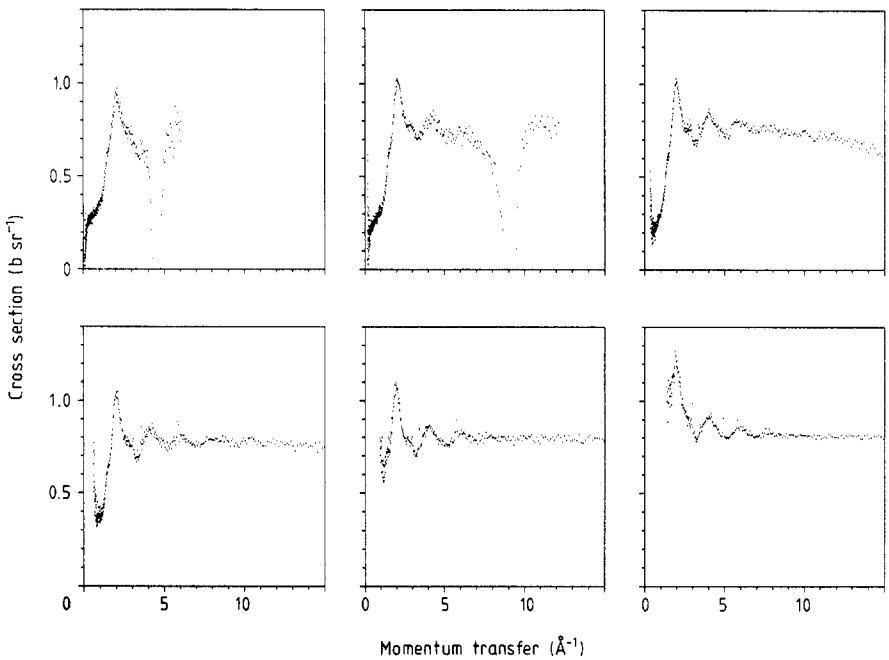

Figure 4. The cross section of molten caesium chloride at 670°C as measured by the detectors at 5°, 10°, 20°, 35°, 58°, and 90°.

3.5. Combining spectra, resolution corrections, and the pair correlation function

A useful way of presenting the corrected data is in the form of the coherent scattering function $F(Q)$,

$$F(Q) = \sum_{\alpha}\sum_{\beta} c_\alpha c_\beta \bar{b}_\alpha \bar{b}_\beta (A_{\alpha\beta}(Q) - 1) = S(Q) - \overline{b^2} \tag{14}$$

as this tends to zero at large Q and thus is in a form that can be Fourier transformed to give the pair correlation function $h_T(r)$. In order to obtain $F(Q)$ over as large a Q-range as possible and with as good statistics as possible we wish to combine the corrected spectra in some way. One approach would be to simply subtract $\overline{b^2}$ from each spectrum and to average them in the regions of overlap. However, small errors in the corrections can mean that the measured $S(Q)$ tends to a value slightly different from $\overline{b^2}$. As $F(Q)$ should tend to zero at large Q it is desirable to subtract the true limiting value of $S(Q)$. Further, this limiting value may be slightly different for the different spectra. This would occur, for example, if the background intensity was slightly attenuated by the sample, or, as we see from figure 2, could be caused by inelasticity effects. Subtracting the same constant from each spectrum would then lead to small discontinuities in the combined $F(Q)$. To overcome these problems we have combined the spectra in this simple manner after subtracting from each a different constant chosen, by a least squares method, so that the spectra match in their regions of overlap and the combined $F(Q)$ has the correct limiting behaviour at high Q.

There is, however, a reason to expect the different spectra to be in less than perfect agreement which we have ignored so far. This is the effect of instrumental resolution

that causes the intensities we have considered to be convoluted with a resolution function, $R(\lambda_e, \lambda'_e)$, that depends on the instrument giving

$$\tilde{I}(\lambda_e) = \int I(\lambda_e) R(\lambda_e, \lambda'_e)\, d\lambda'_e \tag{15}$$

The effect of this convolution is to slightly broaden the structure in the observed intensity. As there is very little structure in the vanadium spectra, apart from Bragg peaks which we ignore anyway, we can ignore the effect of resolution on it. This means that, as we can see from (8), to a good approximation the effect of instrumental resolution is to perform a similar convolution on the $S(Q)$ or $F(Q)$ obtained from each spectrum so we get

$$\tilde{F}(Q) = \int F(Q) R(Q, Q')\, dQ' \tag{16}$$

where we have now written the resolution function, which is in general different for each spectrum, as a function of Q and Q'. $F(Q)$ is related to the total pair correlation function $h_T(r)$ by

$$F(Q) = \frac{4\pi\rho}{Q} \int_0^\infty r\, h_T(r)\, \sin(Qr)\, dr \tag{17}$$

where ρ is the ionic number density and

$$h_T(r) = \sum_\alpha \sum_\beta c_\alpha c_\beta \bar{b}_\alpha \bar{b}_\beta h_{\alpha\beta}(r) \tag{18}$$

where $h_{\alpha\beta}(r) = g_{\alpha\beta}(r) - 1$ and $4\pi r^2 \rho c_\beta g_{\alpha\beta}(r)\, dr$ is the mean number of ions of type β centred in a shell of thickness dr and radius r about an ion of type α. We can therefore write

$$\tilde{F}(Q) = \int R(Q, Q')\, 4\pi\rho \int r^2 h_T(r) \frac{\sin Q'r}{Q'r}\, dr\, dQ' = 4\pi\rho \int r^2 h_T(r) R(Q, r)\, dr \tag{19}$$

where

$$R(Q, r) = \int R(Q, Q') \frac{\sin Q'r}{Q'r}\, dQ'. \tag{20}$$

If we determine $h_T(r)$ not by Fourier transformation of $F(Q)$ but by some method in which $h_T(r)$ is varied until the $\tilde{F}(Q)$ produced by equation (19) are in satisfactory agreement with all the experimental data we can take into account the effects of resolution and obtain one $h_T(r)$ function and, by Fourier transformation of it, one $F(Q)$. This is rather simpler than methods for deconvolving the resolution function entirely in Q-space (Howells 1985). The method we chose to obtain $h_T(r)$ was an adaption of the maximum-entropy method of Root *et al* (1986) which we describe in Appendix 2. For LAD the resolution function is approximated by a Gaussian in time of flight, or λ_e, with a width proportional to the time of flight (Howells 1985).

$$R(\lambda_e, \lambda'_e) = (\Gamma/\lambda_e\sqrt{\pi}) \exp[-\Gamma^2(1 - \lambda'_e/\lambda_e)^2] \tag{21}$$

where Γ is related to the full width at half maximum (FWHM) of the Gaussian by

$$\Gamma^2 = 4 \ln 2/(\text{FWHM}/\lambda_e)^2 \tag{22}$$

and the widths are given by $\text{FWHM}/\lambda_e \simeq 0.11$ (5°), 0.06 (10°), 0.028 (20°), 0.017 (35°) and 0.012 (58° and 90°). At the higher angles the Gaussian form is only approximate but as the resolution function is much narrower at these angles and so resolution is not very important for liquid samples we consider it a good enough approximation for our purposes. It is easily shown that

$$R(Q, Q') = \frac{\Gamma Q}{Q'^2 \sqrt{\pi}} \exp[-\Gamma^2 (1 - Q/Q')^2] \tag{23}$$

so

$$R(Q, r) = \frac{\Gamma Q}{\sqrt{\pi}} \int \frac{1}{Q'^2} \frac{\sin Q' r}{Q' r} \exp[-\Gamma^2 (1 - Q/Q')^2] \, dQ' \tag{24}$$

This integral was performed numerically.

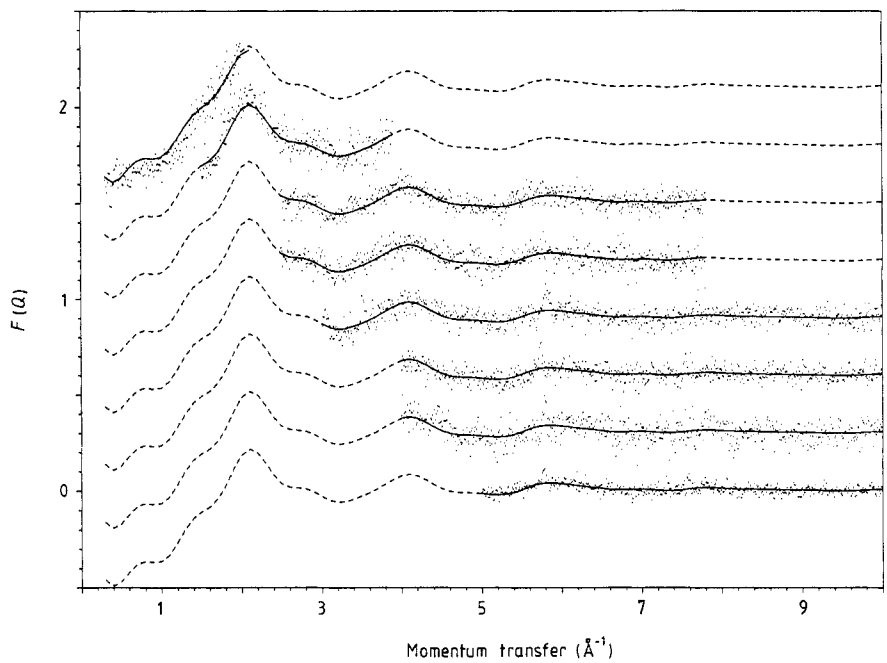

Figure 5. The total structure factor for CsCl at 670°C compared with the data measured by different detectors. The full curves are the resolution broadened function, the broken curves are the unbroadened structure factor and the points are the experimental data.

In figure 5 we compare the individual spectra with the $F(Q)$ and resolution-broadened $\tilde{F}(Q)$ obtained using this method. It is clear that the effect of instrumental resolution, which is largest for the lowest angle detector, is small although not completely negligible. However given the statistical accuracy of this experiment it is not really necessary to include it and we would have done just as well by simply taking

the mean of the spectra. The structure in $F(Q)$ at low Q should not be considered significant. As is clear from the figure this is well within the statistical errors, which are particularly large at low Q and is just an artefact of the process by which we obtained $F(Q)$. This is not really a failure of the method: with better statistics we would expect better results.

4. Results and discussion

The data at 670°C are compared with that obtained on D4 in figure 6. Apart from a possible small systematic deviation the agreement is good and certainly within the statistics. Recent analysis (McGreevy 1988) of the D4 data using the Reverse Monte Carlo technique (Pusztai and McGreevy 1988) suggests that this systematic deviation is due to errors in the D4 data rather than the current data.

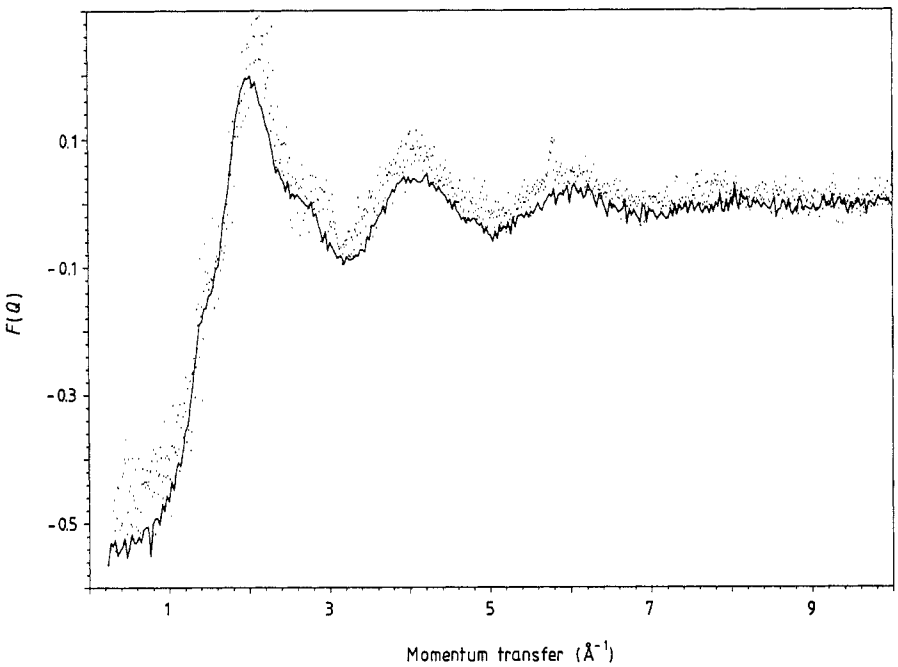

Figure 6. The total structure factor for molten caesium chloride at 670°C as measured using LAD (points) compared with that at 685°C measured using D4 (curve).

The results obtained for the sample at the two temperatures are shown in figure 7. The line is the result from our maximum-entropy procedure while the dots represent the experimental data when the eight spectra have been combined by averaging in the regions of overlap. We see that there appears to be some change in $F(Q)$ with temperature. The value of $F(0)$ increases with temperature; this is to be expected from the change in the compressibility of the salt which gives the theoretical values $F(0) = -0.55$ at 670°C and -0.48 at 970°C. The first peak in $F(Q)$ is not so sharp at the higher temperature. The results, together with the values of $F(0)$ derived from compressibility data, are consistent with $F(Q)$ scaling with the density.

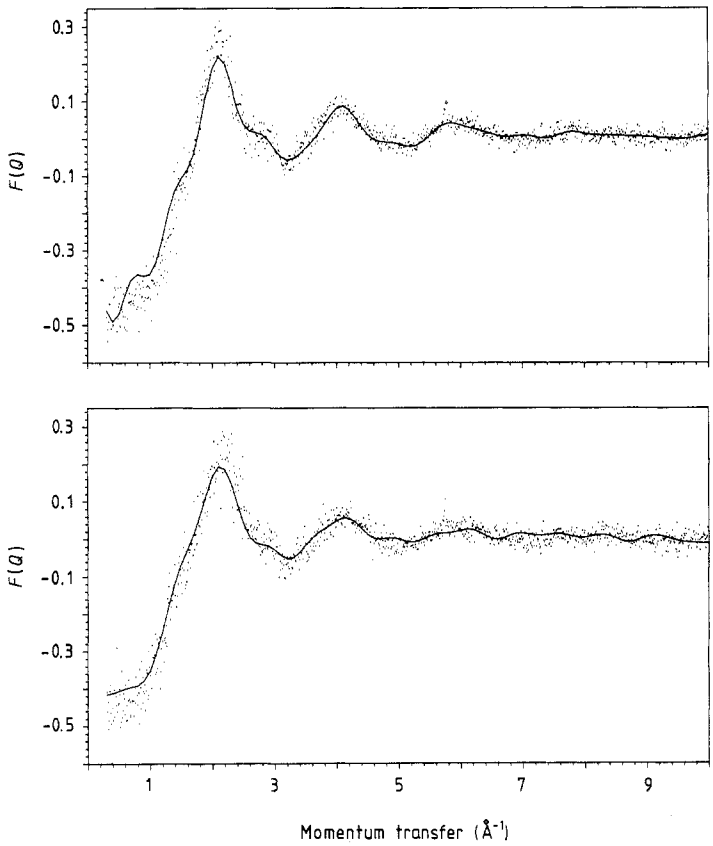

Figure 7. The total structure factor for molten caesium chloride at 670°C (top) and 970°C (bottom).

In figure 8 we show the pair correlation functions. To get some idea of the accuracy of these we have obtained $h_T(r)$ for the lower temperature using several methods: the maximum-entropy method outlined above, a direct Fourier transformation of the combined spectra; and the MAXENTS method of Soper (1986) which is another maximum-entropy-related method, although one that does not include the effects of instrumental resolution. The different methods give answers that are all in fairly good agreement.

The second part of the figure shows the $h_T(r)$ obtained at the two temperatures and from the D4 data. These are in as good agreement as those shown in the first part of the figure so we see that there is no significant change in our measured $h_T(r)$ with temperature.

5. Conclusions

We have developed a procedure for the analysis of LAD data that deals with some of the new problems involved with this type of diffractometry and that produces results that are in good agreement with those obtainable with conventional reactor-based

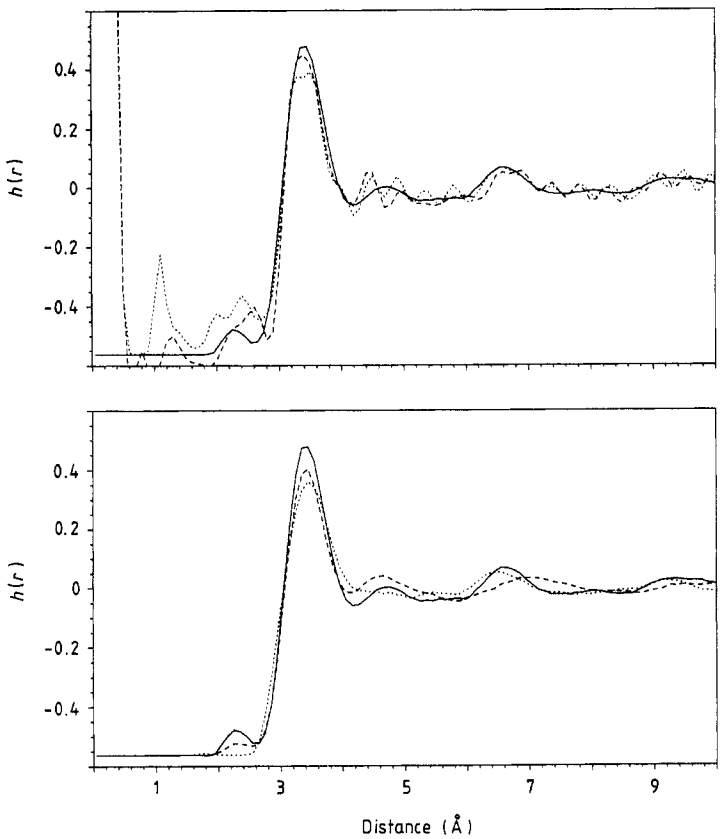

Figure 8. Pair correlation functions. Top: For the sample at 670°C obtained using the procedure described in the text (short dashes), by Fourier transformation (long dashes) and using the MAXENTS program (curve). Bottom: At 670°C (curve), at 685°C from the D4 data (long dashes) and at 970°C (short dashes).

diffractometers. The statistical accuracy of the data we show is very poor because it was obtained soon after ISIS started running and so is, perhaps, not the best test of our methods. However, they have since been applied to much better data and have allowed the technique of isotopic substitution to be successfully applied (Howe *et al* 1989).

We expect that new methods of determining the pair correlation function that avoid Fourier transformation of the experimental data, such as the Reverse Monte Carlo method or Soper's 1D Monte Carlo method (Soper 1987) will be readily adaptable to use our method of including instrumental resolution in the analysis and will be an improvement over the maximum entropy method we have used here.

The only conclusion that can be drawn concerning the temperature dependence of the structure of molten caesium chloride is that although the density changes by 13% between 670°C and 970°C there is little, if any, change in the local structure as described by the pair correlation function. This is consistent with the Raman scattering results (Fairbanks 1987) which show that while the intensity of scattering increases linearly with temperature in the same range, there is no shape in the change of the spectrum.

Appendix 1. Inelasticity corrections

As the manner of calculation is similar to that of Powles (1973) we feel it unnecessary to give full details here and so restrict ourselves to presentation of the results of the series expansions. The reader who wishes to reproduce the calculation is referred to Powles (1973) or to Howe (1987) where our working is given in detail.

We wish to expand the integral in (9) and start by expanding

$$S(Q,\omega) = S(Q_e,\omega) + \left(\frac{\partial S}{\partial(Q^2)}\right)(Q^2 - Q_e^2) + \left(\frac{\partial^2 S}{\partial(Q^2)^2}\right)\frac{(Q^2 - Q_e^2)^2}{2} + \ldots. \tag{A1.1}$$

For convenience we introduce the dimensionless quantities

$$x = m\omega/\hbar k_e^2 \qquad f = d_1/(d_1 + d_2). \tag{A1.2}$$

Expanding to second order in x we find

$$\begin{aligned} k_e/k &= \lambda/\lambda_e = 1 + (f-1)x + (3/2)(f-1)(2f-1)x^2 + \ldots \\ k/k' &= \lambda'/\lambda = 1 + x + [(4f-1)/2]x^2 + \ldots \\ k'/k_e &= \lambda_e/\lambda' = 1 - fx - [(4f^2 - 3f)/2]x^2 + \ldots \end{aligned} \tag{A1.3}$$

which enable us to expand all the factors in the integrand of (9)

$$k'/k = \lambda/\lambda' = 1 - x + [(3-4f)/2]x^2 + \ldots. \tag{A1.4}$$

The constant C defined by (10) can be expanded to give

$$C = 1 + 2(1-f)x + 2(5f-2)(f-1)x^2 + \ldots. \tag{A1.5}$$

$\phi(\lambda)$ is expanded as a Taylor series about λ_e to give

$$\phi(\lambda)/\phi(\lambda_e) = 1 + (f-1)\phi_1 x + [3(f-1)(f-1/2)\phi_1 + (1/2)(f-1)^2\phi_2]x^2 + \ldots \tag{A1.6}$$

where

$$\phi_1 = \lambda_e\phi'(\lambda_e)/\phi(\lambda_e) \qquad \phi_2 = \lambda_e^2\phi''(\lambda_e)/\phi(\lambda_e) \tag{A1.7}$$

and the primes indicate differentiation. Similarly expanding $\epsilon(k')$ about k_e we get

$$\epsilon(k')/\epsilon(k_e) = 1 - f\epsilon_1 x + [(f^2\epsilon_2 - f\epsilon_1)/2]x^2 + \ldots \tag{A1.8}$$

where

$$\epsilon_1 = k_e\epsilon'(k_e)/\epsilon(k_e) \qquad \epsilon_2 = k_e^2\epsilon''(k_e)/\epsilon(k_e). \tag{A1.9}$$

Finally, the expansion of $Q^2 - Q_e^2$ is

$$Q^2 - Q_e^2 = Q_e^2(1-2f)x + [k_e^2 - Q_e^2(3f^2 - 3f + 1/2)]x^2 + \ldots. \tag{A1.10}$$

Substituting into (A1.1) gives

$$S(Q,\omega) = S(Q_e,\omega) + Q_e^2(1-2f)S'x + \{[k_e^2 - Q_e^2(3f^2-3f+1/2)]S' + Q_e^4(2f^2-2f+1/2)S''\}x^2 + \ldots. \tag{A1.11}$$

We are now in a position to evaluate the integral in (9). The zeroth-order term in x is simply

$$\int d\omega\, S(Q_e,\omega) = S(Q_e) \tag{A1.12}$$

which is exactly what we wish to determine. The higher-order terms are the corrections that must be made to the experimentally determined cross section to obtain this. For these we require the moments of $S(Q,\omega)$ which are

$$\begin{aligned} S_1(Q) &= \int_{-\infty}^{\infty} d\omega\, \omega S(Q,\omega) = \sum_\alpha \frac{c_\alpha \overline{b_\alpha^2} \hbar Q^2}{2M_\alpha} \\ S_2(Q) &= \int_{-\infty}^{\infty} d\omega\, \omega^2 S(Q,\omega) = \sum_\alpha c_\alpha \overline{b_\alpha^2}\left(\frac{k_B T Q^2}{M_\alpha} + \frac{\hbar^2 Q^4}{4M_\alpha^2} + \ldots\right) \end{aligned} \tag{A1.13}$$

where k_B is the Boltzmann constant and T is the temperature. The first-order term to the correction is thus

$$\begin{aligned} P_1(Q_e) &= \int d\omega \left([\phi_1(f-1) - f\epsilon_1 + 3f - 4]S(Q_e,\omega) + Q_e^2(1-2f)\frac{\partial S}{\partial (Q^2)}\right)x \\ &= \frac{m}{\hbar k_e^2}\left([(f-1)\phi_1 - f\epsilon_1 + 3f - 4]S_1(Q_e,\omega) + Q_e^2(1-2f)\frac{\partial}{\partial (Q^2)}S_1(Q_e,\omega)\right) \\ &= \frac{m}{\hbar k_e^2}[(f-1)\,\phi_1 - f\epsilon_1 + f - 3]\frac{\hbar Q_e^2}{2}\sum_\alpha \frac{c_\alpha \overline{b_\alpha^2}}{M_\alpha} \\ &= 2[(f-1)\phi_1 - f\epsilon_1 + f - 3]\sin^2(\theta/2)\sum_\alpha c_\alpha \overline{b_\alpha^2}\frac{m}{M_\alpha} \end{aligned} \tag{A1.14}$$

which agrees with the result of Powles; the second-order term is

$$\begin{aligned} P_2(Q_e) = \{&k_B T/2E + (k_B T/E)\sin^2(\theta/2)[(8f-9)(f-1)\phi_1 - 3f(2f-3)\epsilon_1 \\ &+ 2f(1-f)\phi_1\epsilon_1 + (1-f)^2\phi_2 + f^2\epsilon_2 + 3(4f-5)(f-1)]\}\sum_\alpha c_\alpha \overline{b_\alpha^2}\frac{m}{M_\alpha} \\ &+ 2\sin^2(\theta/2)\{1 + \sin^2(\theta/2)[(4f-7)(f-1)\phi_1 + f(7-2f)\epsilon_1 \\ &+ 2f(1-f)\phi_1\epsilon_1 + (1-f)^2\phi_2 + f^2\epsilon_2 + (2f^2-7f+8)]\}\sum_\alpha c_\alpha \overline{b_\alpha^2}\frac{m^2}{M_\alpha^2} \end{aligned} \tag{A1.15}$$

where E is the energy of the incident neutrons.

The series expansions and manipulations involved in this calculation were performed and checked using the REDUCE algebraic manipulation program on a VAX 11/780 of the Oxford University Computing Service.

Appendix 2. Applying the maximum-entropy method

We base this on the method of Root *et al* (1986). They define the information entropy to be

$$H = -4\pi \int \mathrm{d}r\, r^2 g(r)\,(\ln g(r) - 1) \tag{A2.1}$$

which is written in a discrete form as

$$H = -4\pi \sum_{i=1}^{N_r} \Delta r\, r_i^2 g_i\,(\ln g_i - 1) \tag{A2.2}$$

where N_r is the number of points in r-space. If $g(r)$ is actually a neutron-weighted sum, $g_T(r)$, of partial correlation functions, $g_{\alpha\beta}(r)$ defined in an analogous fashion to (18) it is necessary to replace g_i in this equation by g_i/g_∞ where $g_\infty = \lim_{r\to\infty} g(r)$. The χ^2 constraint is, in our case,

$$\frac{1}{N-1} \sum_n \sum_i (E_{ni} - \tilde{F}_{ni})^2/\sigma_{ni}^2 = 1 \tag{A2.3}$$

where n labels the spectrum, i labels the point within the spectrum, and N is the total number of data points for all spectra. E_{ni} are the experimental data, the σ_{ni} are the standard deviations of the points and $\tilde{F}_{ni}$ is given by (see (19))

$$\tilde{F}_{ni} = 4\pi\rho \sum_k \Delta r\, r_k^2 (g_k - 1) R_{nik} \tag{A2.4}$$

where R_{nik} is $R(Q_i, r_k)$ for the nth spectrum. We maximise H using the method of undetermined Lagrange multipliers so we require that

$$\frac{\partial}{\partial g_j}\left[-4\pi \sum_{i=1}^{N_r} \Delta r\, r_i^2 \frac{g_i}{g_\infty}\left(\ln \frac{g_i}{g_\infty} - 1\right) - \frac{\Lambda}{N-1} \sum_n \sum_i (E_{ni} - \tilde{F}_{ni})^2/\sigma_{ni}^2\right] = 0 \tag{A2.5}$$

where Λ is a Lagrange multiplier. From (A2.4) we see that

$$\partial \tilde{F}_{ni}/\partial g_j = 4\pi\rho \Delta r\, r_j^2 R_{nij} \tag{A2.6}$$

so that

$$g_j = g_\infty \exp\left(\frac{2\rho\Lambda g_\infty}{N-1} \sum_n \sum_i (E_{ni} - \tilde{F}_{ni})/\sigma_{ni}^2 R_{nij}\right). \tag{A2.7}$$

Substituting (A2.4) into this gives a set of coupled equations in the g_j which, for a given value of Λ, may be solved by, for example, the Newton–Raphson method. The procedure, then, is to choose a value of the Lagrangian multiplier Λ; solve (A2.7) for the g_j by repeated iteration, calculate the value of the constraint function in (A2.3); if this is not sufficiently close to 1 then adjust the value of the Lagrange multiplier and repeat the process until either the constraint is satisfied or no progress is being made in approaching it. In practice the values σ_{ni} are not known exactly so it is sufficient to

run the programme until there is no further improvement in the value of the constraint function. This differs from the method of Root *et al* (1986) in solving in r-space rather than Q-space; this is necessary if we are to include the resolution.

We have assumed in the above that the E_{ni} are data points of spectra from which the limiting value has already been subtracted. If that is not the case we can easily introduce a constant c_n for each spectrum and replace E_{ni} in (A2.3) by $E_{ni} - c_n$. We choose c_n to minimise χ^2 for each spectrum so that

$$c_n = \left(\sum_k (E_{nk} - \tilde{F}_{nk})/\sigma_{nk}^2\right)\left(\sum_k 1/\sigma_{nk}^2\right)^{-1}. \tag{A2.8}$$

This term must then be inserted in (A2.5).

References

Bischoff F G, Yeater M L and Moore W E 1972 *Nucl. Sci. Eng.* **48** 226

Bunten R A J, McGreevy R L, Mitchell E W J, Raptis C, and Walker P J 1984 *J. Phys. C: Solid State Phys.* **17** 4705

Copley J R D 1974 *Comput. Phys. Comm.* **7** 289

Day S E and McGreevy R L 1985 *Phys. Chem. Liq.* **15** 129

Dahlborg U and Kunsch B 1983 *Phys. Chem. Liq.* **12** 237

Fairbanks M C 1987 *DPhil Thesis* University of Oxford

Fairbanks M C and McGreevy R L 1989 *Phys. Chem. Liq.* at press

Howe M A 1987 *DPhil Thesis* University of Oxford

Howe M A and McGreevy R L 1988 *Phil. Mag.* B **58** 485

Howe M A, Wormald C J and Neilson G W 1989 *Mol. Phys.* at press

Howells W S 1980 *Rutherford Laboratory Report* RL-80-017

——1984 *Nucl. Instrum. Methods* A **223** 141

——1985 *Nucl. Instrum. Methods* A **235** 553

——1986 *Rutherford Appleton Laboratory Report* RAL-86-042

Howells W S, Price D L and Montague D G 1985 unpublished

ISIS User Guide 1988 *Rutherford Appleton Laboratory Report* RAL-88-033

Janz G J 1967 *Molten Salts Handbook* (New York: Academic)

Locke J, Messoloras S, Stewart R J, McGreevy R L and Mitchell E W J 1985 *Phil. Mag.* B **51** 301

Lovesey S W 1984 *Theory of Neutron Scattering from Condensed Matter* (Oxford: Clarendon)

McGreevy R L 1987 *Solid State Phys.* **40** 247 (New York: Academic)

——1988 Private communication

Mildner D F R and Carpenter J M 1977 *Acta Crystallogr.* A **33** 962

Mildner D F R, Pelizzari C A and Carpenter J M 1977 *Acta Crystallogr.* A **33** 954

Paalman H H and Pings C J 1962 *J. Appl. Phys.* **33** 2635

Placzek G 1952 *Phys. Rev.* **86** 377

Poncet P F J 1977 *ILL Internal Report* 77PO139S

Powles J G 1973 *Mol. Phys.* **26** 1325

Price D L 1982 *IPNS Note* 19 (unpublished)

Pusztai L and McGreevy R L 1988 *Mol. Simulation* **1** 359

Root J H, Egelstaff P A and Nickel B G 1986 *Workshop on Neutron Scattering Data Analysis 1986* (Inst. Phys. Conf. Ser. 81) p 71

Saboungi M-L, Blomquist R, Volin K J and Price D L 1987 *J. Chem. Phys.* **87** 2278

Sears V F 1975 *Adv. Phys.* **24** 1

Soper A K 1986 *Chem. Phys.* **107** 61

——1987 *EPS Conf. Liquids of Small Molecules (Reggio, Calabria)*

——1988 Private communication

Soper A K and Egelstaff P A 1980 *Nucl. Instrum. Methods* **178** 415

Wood N D, Howe R A, Newport R J and Faber J Jr 1988 *J. Phys. C: Solid State Phys.* **21** 669

Wright A C, Yarker C A and Johnson P A V 1985 *J. Non-Cryst. Solids* **76** 333

Yarnell J L, Katz M J, Wenzel R G and Koenig S H 1973 *Phys. Rev.* A **7** 2130